# Edge Effects in a Strongly Coupled Dipole Element Array in Triangular Lattice

**C. I. Kolitsidas and B. L. G. Jonsson**
Electromagnetic Engineering, School of Electrical Engineering
KTH Royal Institute of Technology, Sweden
(*Invited Paper*)

**Abstract**— In this work the focus is on the impact of edge effects in the equilateral triangular lattice of a strongly coupled dipole antenna array. A novel wideband strongly coupled, single polarized, dipole element is designed and studied in a triangular grid. The antenna element operates in 6 : 1 bandwidth ratio. Our analysis for the edge effects is based the finite × infinite approach with multiple rows taken into account in order to capture the effects on the different edges that appear in triangular grids. The effects at the E-edge are studied as it is the plane where the currents are truncated. At the E-edge the variation on the behavior is mainly due to lack of closely coupling fields. Using the finite × infinite approach the variations along the E-edge of the array are studied for both rectangular and triangular grid. Finally, periodic resistive loading was used on the dipoles to dissipate the waves produced from the edges and smooth the impedance behavior along the array row.

## 1. INTRODUCTION

Wideband antenna arrays for wireless communications is a topic that has attracted a lot of interest over the last few decades. Future wireless base stations are envisioned to support all commercially available bands. Furthermore, it is expected to offer advanced coverage characteristics, like dedicated user beams. It is the path towards implementing a multi-user multiple input multiple output (MU-MIMO) system for commercial applications. This generates the need for a wideband and wide-scan antenna array suitable for base station applications.

Over the last decade, a new class of wideband antenna array systems has been developed that is able to utilize strong inter-element coupling. Their ability to operate in such large bandwidth comes from the fact that the array allows almost continuous currents that results in greater operational bandwidths. It is the implementation of the Wheeler's concept of current sheet array [1], and it has developed into two major wideband antenna array technologies: The capacitively coupled dipoles [2], and connected dipoles/slots [3]. It was shown [2], that these elements are able to provide wideband (5 : 1) performance while keeping a relatively low profile ($d \approx \lambda_{high\ freq}/2.5 - \lambda_{high\ freq}/3$, $d$ is the distance from the ground plane to the radiating structure). It is an attractive approach with the possibility for communication applications. In the case of base station application this type of array can be an ideal candidate and due to the limited space at the base station the mid-sized array is in need to be investigated.

An important factor that appears during the finite array design procedure is the performance variations of the elements with respect to their position in the array. These variations are mainly caused by the "edge effects" in the finite array. Thus it is expected that the outer elements in the finite array will have degraded performance when compared with the central array elements. Another important factor that impacts the scanning performance of the array is the array lattice selection. An eigen current approach was used in [4] to capture the edge effects on a finite array. A study for edge element evaluation at tapered slot antennas placed in triangular grid was conducted in [5]. Here, it is worth mentioning that tapered slot antennas also rely on strong interelement coupling to eliminate undesired structural resonances and achieve wideband performance. The size of the array needed in order to behave close to the unit cell analysis was the outcome of the study in [6].

In our previous studies, we have investigated the inter-element coupling [7], to enhance bandwidth performance and edge elements optimization [8], in order to compensate truncation effects at the edge elements. Recently, a general measure of the performance of planar arrays backed by a metallic reflector was derived: The array figure of merit [9]. It provides the possibility to connect physical and electrical characteristics that result in a measure of the arrays performance. In its simple form contains the distance ($d$) from the ground plane as the main physical characteristic which is the limiting factor of unidirectional planar arrays.

In the present work the edge effects at the E-edge of strongly coupled dipole with capacitive loading array will be studied. A comparison between the behavior in rectangular and triangular grids is made for low and high impedance loading on each element. The impedance loading is used to dissipate the waves from the edges and create a smooth active input impedance variation.

## 2. UNIT CELL DESIGN AND ARRAY CONFIGURATION

The geometry of the unit cell design of closely spaced dipoles is depicted in Fig. 1. The dipole has been capacitively loaded with a small inter-element gap $2 \cdot \delta$, where $\delta = 0.6\,\text{mm}$, and an additional parasitic patch in the back of the dipole between the arms as can be seen in Fig. 1(c). The small gap in between the elements significantly increases the inter-element coupling between the adjacent dipole arms. The capacitive loading of the dipole is depicted as schematic in Fig. 1(d). The latter is required to counteract the inductive behavior of the ground plane as is indicated in [2, 7]. Furthermore the height between the dipoles and the ground plane is chosen to be $\lambda_{high\ freq}/2.5$ in order to avoid a zero in the broadside direction at the high end of the frequency band. Also, in order to increase the bandwidth towards the lower end of the frequency band we have loaded the dipole arms with a T-slot increasing the current path. The dipole is fed by a balanced co-planar strip line ($s = 0.3\,\text{mm}$ $C_l = 2\,\text{mm}$) which is tapered to a wide microstrip line ($w = 11\,\text{mm}$, $l = 9.52\,\text{mm}$). For the T-slot the dimensions are: $w_{T1} = 2\,\text{mm}$, $w_{T2} = 2\,\text{mm}$ and $T_l = 8\,\text{mm}$. The unit cell dimensions are chosen $\lambda_{high\ freq}/2$ in order to be below at the grading lobe limit for the fundamental Floquet mode. The dipole is designed in Rogers RO4003 ($\epsilon_r = 3.55$, $\tan\delta = 0.0027$ & $h = 1.52\,\text{mm}$) printed circuit board (PCB). Finally, the dipole is loaded with a WAIM (Wide Angle Impedance Matching) layer ($\epsilon_r = 2$) that improves bandwidth and scanning performance. The feeding of the array element will be completed with a commercial BalUn/$4:1$ impedance transformer from an unbalanced CPW (Co-Planar Waveguide) to a balanced CPS (Co-Planar Strips) line. The behavior of the VSWR of the array's unit cell is depicted in Fig. 2(a) where we can observe that the operational bandwidth of the array is $6:1$ ratio. In Fig. 2(b) is depicted the computational domain used to evaluate the E-edge effects. We have applied periodic boundary conditions on two rows of the array to capture the E-edge effects. The analysis have been carried out on CST Microwave Studio [10].

The active reflection coefficient $\Gamma(\psi_x, \psi_y)$ of the unit cell takes into account all coupling phenomena that occur in the array. For a given planar rectangular lattice under Floquet excitation is given as in [11]:

$$\Gamma(\psi_x, \psi_y) = \sum_{n=-\infty}^{\infty} S_{mn} \exp\left[-j\left(\frac{d_x(m,n)\psi_x}{a} + \frac{d_y(m,n)\psi_x}{b}\right)\right] \tag{1}$$

where all scattering parameters $S_{mn}$ contribute to the final active reflection coefficient. In detail, $\psi_x$ and $\psi_y$ are the phase differences between the adjacent elements, in our case $\alpha = b = d$ and $d_x(m,n)$, $d_y(m,n)$ are the relative distances along the $x$ and $y$ direction between the $m$th and $n$th element. From the active reflection coefficient of each element in the array the active impedance can be extracted. This is used to evaluate the impedance variations along the E-edge.

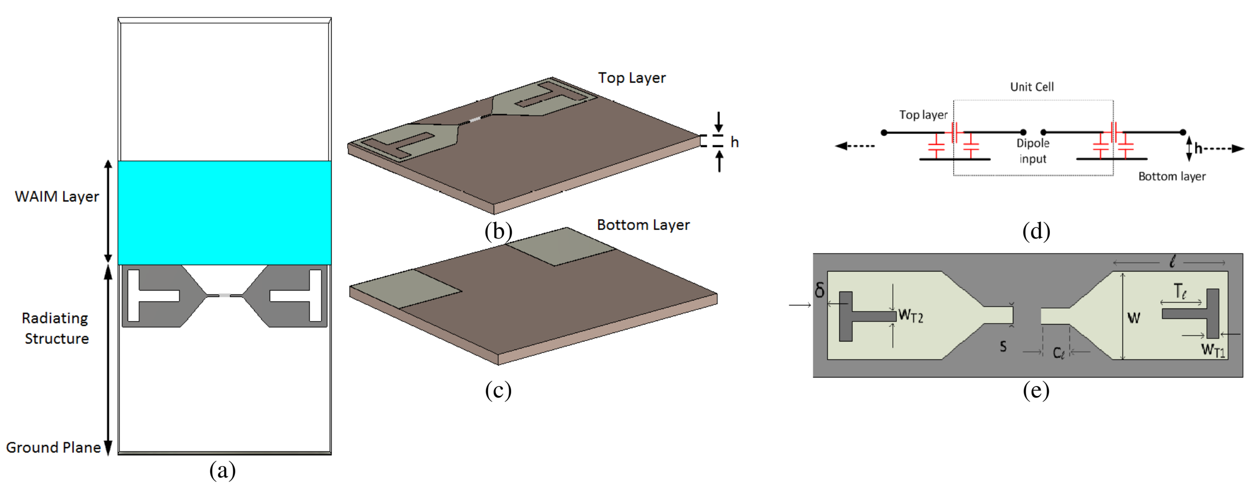


Figure 1: (a) Array unit cell with T-slot loaded dipole and WAIM. (b) Top layer. (c) Bottom Layer. (d) Capacitive dipole loading. (e) Element with corresponding dimensional variables.

## 3. ANALYSIS OF TRUNCATION AND PERIODIC RESISTIVE LOADING

The final current at each element on the finite array is the current from the unit cell analysis with a perturbation current that will be generated from the diffraction of the field at the edges. The edge effects have also been described with a heuristic Gibbsian model [12]. This perturbation on the current at each element will have an impact at the active input impedance of each element. Using the finite $\times$ infinite approach it is possible to isolate the behavior of each edge separately. In this analysis we are focused on the E-edge behavior and the analysis is based on a 12 element linear array, electrical length of $6 \cdot \lambda_{high\ freq}$, that is placed on a rectangular and equilateral triangular lattice. In the case of the triangular grid two rows have been used of the linear array as the computational space (Fig. 2(b)). In order for the finite array to operate as the unit cell we must have as less impedance variations as possible. As part of the analysis two different load impedances have been used, one at 150 Ohms and one at 377 Ohms. The first load impedance offers maximum usable bandwidth on the array element and the second is chosen according to [13] which states that periodic high impedance loading of the array the waves that are produced from the edge effects can be dissipated. This concept is applied here for the first time in a triangular lattice and compared with the behavior of the rectangular lattice.

In Fig. 3(a), the results for the active input impedance with the 150 Ohm load are depicted for the frequency of 3 GHz, whereas at Fig. 3(b) are depicted the for the 377 Ohm active input impedance at the same frequency. It is observed that the there is small difference between the two grids when the load is 150 Ohm but the triangular grid has smoother variation when the load

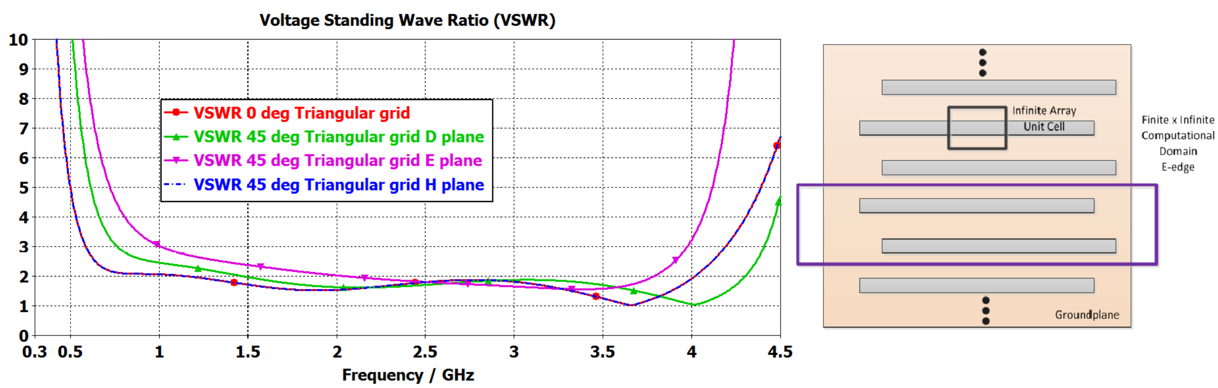


(a) (b)

Figure 2: (a) Active VSWR for different scan angles of the array unit cell placed in a triangular lattice. (b) E-edge computational domain with finite $\times$ infinite approach.

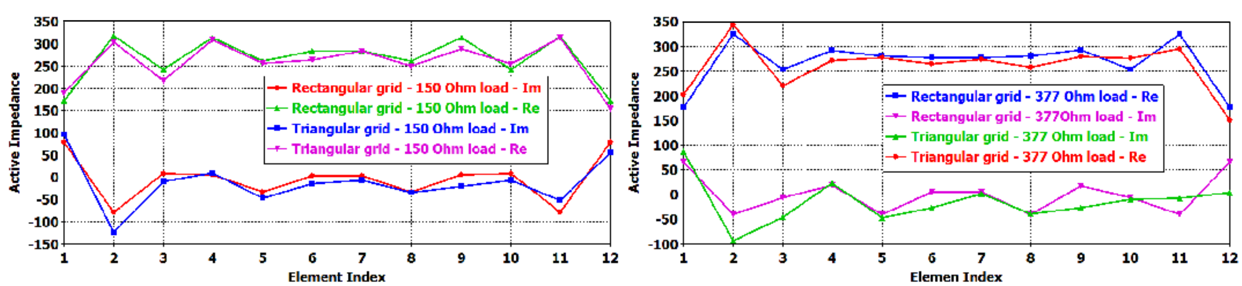


(a) (b)

Figure 3: Active impedance of the elements at 3 GHz with finite $\times$ infinite approach comparison of equilateral and rectangular lattice (a) with 150 Ohm loading and (b) 377 Ohm loading for periodic dissipation of edge effects.

Table 1: Root mean square error.

| 150 Ohm loading | | | | 377 Ohm loading | | | |
|---|---|---|---|---|---|---|---|
| Real | | Imaginary | | Real | | Imaginary | |
| Rect. | Triang. | Rect. | Triang. | Rect. | Triang. | Rect. | Triang. |
| 28.02% | 26.28% | 18.29% | 16.55% | 13.90% | 18.11% | 23.99% | 23.71% |

impedance changes to 377 Ohm. Also, if one compares the behavior of the two load impedances, it is clear that the high load impedance has better — more smooth behavior, especially at the 8 central dipoles. A summary with the root mean square error of the two configurations can be found on Table 1. The dissipation of edge generated waves with high impedance comes at the cost of the operational bandwidth shrinkage. This happens, as the matching impedance that is used is the the peak of the real part of the strongly coupled dipole and not close to the mid point of 150 Ohms.

## 4. CONCLUSION

This work is focused on the impact of edge effects in the equilateral triangular lattice of a strongly coupled antenna array. A novel wideband strongly coupled, single polarized, dipole element is designed and studied in a triangular grid. The antenna element operates in 6 : 1 bandwidth ratio. Our analysis for the edge effects is based the finite × infinite approach with multiple rows taken into account in order to capture the effects on the different edges that appear in triangular grids. The effects at the E-edge are studied for both rectangular and triangular grid and compared. A periodic resistive loading on the dipoles was used to dissipate the waves produced from the edges and smooth the impedance behavior along the array row. These results are compared with the case without resistive loading. This final approach produced improved results for the triangular grid but with the penalty of operational bandwidth shrinkage.

## ACKNOWLEDGMENT

This work was financially supported by The Swedish Governmental Agency for Information Systems (VINNOVA) within the VINN Excellence center, Chase stage III through the research project Next Generation Antenna Arrays.

## REFERENCES

1. Wheeler, H., "Simple relations derived from a phased array antenna made of an infinite current sheet," *IEEE Trans. on Antennas and Propag.*, Vol. 13, No. 4, 506–514, Jul. 1965.
2. Munk, B. A., *Finite Arrays and FSS*, Wiley-Inter-Science, New York, 2003.
3. Neto, A., D. Cavallo, G. Gerini, and G. Toso, "Scanning performances of wide band connected arrays in the presence of a backing reflector," *IEEE Trans. on Antennas and Propag.*, Vol. 57, No. 10, 3092–3102, Oct. 2009.
4. Bekers, D. J., J. L. Eijndhoven, and A. G. Tijhuis, "An eigencurrent approach of finite arrays of electromagnetically characterized elements," *Radio Sci.*, Vol. 44, RS2S90, 2009.
5. Ellgardt, A. and M. Norgren, "A study of edge effects in triangular grid tapered slot arrays using coupling coefficients," *Radio Sci.*, Vol. 4, RS2005, 2010.
6. Holter, H. and H. Steyskal, "On the size requirement for finite phased array models," *IEEE Trans. on Antennas and Propag.*, Vol. 50, No. 6, 836–840, Jun. 2002.
7. Kolitsidas, C. I. and B. L. G. Jonsson, "Investigation of compensating the ground plane effect through array's interelement coupling," *Proceedings of 7th European Conference on Antennas and Propagation (EuCAP)*, 1221–1224, Gothenburg, Sweden, Apr. 2013.
8. Kolitsidas, C. I. and B. L. G. Jonsson, "A study of partial resonance control for edge elements in a finite array," *PIERS Proceedings*, 253–256, Stockholm, Sweden, Aug. 12–15, 2013.
9. Jonsson B. L. G., C. I. Kolitsidas, and N. Hussain, "Array antenna limitations," *IEEE Antennas and Wireless Propagation Letters*, Vol. 12, 1539–1542, 2013.
10. CST *Microwave studio®*, 2012.
11. Bhattacharyya, A. K., *Phased Array Antennas*, Wiley-Inter-Science, New York, 2005.
12. Hansen, R. C. and D. Gammon, "A Gibbsian model for finite scanned arrays," *IEEE Trans. on Antennas and Propag.*, Vol. 44, No. 2, 243–248, Feb. 1996.
13. Neto, A., D. Cavallo, and G. Gerini, "Edge-born waves in connected arrays: A finite × infinite analytical representation," *IEEE Trans. on Antennas and Propag.*, Vol. 59, No. 10, 3646–3657, Oct. 2011.